

Carbon *K*-shell x-ray and Auger-electron production in hydrocarbons and carbon oxides by 0.6–2.0-MeV protons

R. P. Bhalla* and F. D. McDaniel

Department of Physics, North Texas State University, Denton, Texas 76203

G. Lapicki

Department of Physics, East Carolina University, Greenville, North Carolina 27858

(Received 17 September 1986)

Carbon *K*-shell x-ray and Auger-electron-production cross sections are reported for 0.6–2.0-MeV protons incident on CH₄ (methane), C₂H₂ (acetylene), *n*-C₄H₁₀ (normal butane), *i*-C₄H₁₀ (isobutane), C₆H₆ (benzene), CO, and CO₂. A variable-geometry end-window proportional counter with an alternate procedure for the determination of its transmission was used in collection of the x-ray data. A constant-energy-mode $\pi/4$ parallel-plate electrostatic analyzer served in the detection of Auger electrons. *K*-shell Auger-electron-production cross sections are compared with the predictions of the first Born theory and the perturbed-stationary-state theory which accounts for energy-loss, Coulomb deflection, and relativistic effects (ECPSSR). These data show fair agreement with the ECPSSR theory when the chemical shifts, of the carbon *K*-shell binding energy in molecules, are included in the calculations. This agreement is even better after effects of intramolecular scattering are considered. Validity of the geometrical model by Matthews and Hopkins [Phys. Rev. Lett. **40**, 1326 (1978)] is established after a scrutiny of the inelastic cross sections for scattering of Auger-electrons within the molecule and their effective dislocation out of the detector's window. The x-ray cross sections show particularly strong variations with the target molecular species because of additional changes due to modifications in the fluorescence yields for molecular carbon. The correlation of these changes with the molecular character of carbon and a scaling procedure for the fluorescence yields in molecules will be discussed elsewhere.

I. INTRODUCTION

K-shell fluorescence yields as well as x-ray cross sections have been found to vary with the chemical environment. This was first discovered by Harrison, Tawara, and de Heer¹ in electron bombardment of carbon-bearing molecules. The relative x-ray yields were found to vary in magnitude by up to 35%. Bissinger *et al.*² have also seen that the fluorescence yields and relative x-ray yields for carbon and oxygen bombarded by 2.0-MeV protons were indeed changed by the chemical environment. Auger-electron production is also affected by the type of molecular target. Matthews and Hopkins³ have measured Auger-electron cross sections for a number of symmetric molecules and found that the carbon *K*-shell Auger-electron cross sections decreased by 32% from CH₄ to CCl₄. They interpreted this change in terms of an inelastic scattering of Auger electrons during transit through the surrounding chlorine atoms. Chaturvedi *et al.*⁴ measured the fluorine *K*-shell Auger-electron-production cross sections in a series of fluorine-bearing gases. They observed a 10% smaller cross sections in SF₆ than the average cross section in the remaining gases.

Chemical effects have been also seen in solid targets. Endo *et al.*⁵ used photon and electron beams on a series of fluorides. The relative intensity of the first satellite to the diagram line was found to change systematically with the Pauling bond ionicity of the investigated fluorides. Watson *et al.*⁶ used beams of 2.0-MeV/u oxygen and

neon ions to produce sulfur *K α* x-ray emission in Na₂S, ZnS, S₈, and Na₂SO₄. They have observed an easily measurable chemical effect in the height distribution of the *K α* x-ray satellites from the sulfur compounds. Neither Endo *et al.* nor Watson *et al.* studied x-ray-yield variations in their solid compounds.

In this investigation we report measurements of the carbon *K*-shell x-ray and Auger electron cross sections by 0.6–2.0-MeV H⁺ ions incident on CH₄, C₂H₂, *n*- and *i*-C₄H₁₀, C₆H₆, CO, and CO₂. Changes of our Auger-electron data for C₂H₂ relative to CH₄ agree, while a 20% decrease of Auger-electron cross sections for CO₂ disagrees with those published earlier by Toburen.⁷ He saw only an 11% decline in going from CH₄ to CO₂ and indicated, however, that the data for carbon oxides were not taken under the same conditions as for methane and acetylene. The basic purpose of our paper is to assess the influence of chemical milieu of carbon on its *K*-shell ionization cross sections and to report *both* x-ray and Auger-electron-production cross sections for the identical collisions with molecular targets. We are aware of only two instances⁸ in which x-ray and Auger-electron data were measured at the same laboratory for identical collision systems.

The experimental arrangement designed for the measurement of these cross sections is outlined in Sec. II. Data analysis is discussed in Sec. III. Carbon *K*-shell x-ray and Auger-electron cross sections are presented in Sec. IV: our x-ray cross sections are compared with the data

of others,⁹⁻¹¹ and the empirical ionization cross sections are compared with calculations of the first Born theory¹² and the ECPSSR theory.¹³ The acronym ECPSSR stands for the projectile's energy loss and Coulomb deflection and for perturbed-stationary-state and relativistic effects in the inner shell of the target atom.

II. EXPERIMENTAL ARRANGEMENT

A schematic drawing of the apparatus used to measure the x-ray and Auger electron cross sections is shown in Fig. 1. The proton beam was supplied by a 2.5-MV Van de Graaff accelerator at North Texas State University and was collimated by two circular apertures C_1 and C_2 of diameters 0.8 and 1.0 mm, respectively separated by 1.0 m. All collimators were machined to thin edges so as to minimize the slit-edge scattering. The beam was then passed through a clean-up collimator C_3 of diameter 1.5 mm before entering the target gas cell. A pair of electrostatic deflection plates was inserted between apertures C_2 and C_3 to deflect the proton beam in the horizontal plane. The beam, after passing through a differentially pumped gas cell, was collected in a Faraday cup biased at +90 V to prevent the escape of secondary electrons. The proton current was monitored by a current integrator. All gases were of ultrahigh purity (99.9% or better). Pressure in the gas cell was monitored by a Baratron capacitance manometer. The entire apparatus was surrounded with a Co-Netic magnetic shielding material to reduce the effect of the earth's and other magnetic fields. X rays were detected by a variable-geometry proportional counter¹⁴ of the end-window type placed at an angle of 150° with respect to the incident beam direction.

A polypropylene window was used in the proportional counter for the detection of carbon K -shell x rays. An ultrathin section of polypropylene, sandwiched between two stainless-steel grids of 50 wires per inch, was epoxied to a stainless-steel disc using a conductive silver epoxy.¹⁵ This assembly was then placed in the opening of the proportional counter. The counter gas used was P10 (90% argon and 10% methane). The anode was a 0.0025-cm-diameter tungsten wire. The proportional counter was energy calibrated by exposing titanium and vanadium targets on thin self-supporting carbon foil to the proton beam and by measuring the carbon K -shell, titanium L -shell, and vanadium L -shell x rays.

Auger electrons were detected by a $\pi/4$ parallel-plate electrostatic analyzer placed at an angle of 90° with respect to the beam direction. Our electrostatic analyzer has been discussed elsewhere¹⁶ so that only a brief descrip-

tion of its use will be given here. The analyzer was operated in the constant-transmission-energy mode. Two einzel lenses were used in conjunction with an intermediately located deceleration arrangement to efficiently manipulate the energy resolution, intensity, and energy of an electron beam prior to the analyzer entrance slit. This system decelerated all electrons to be analyzed to a selectable transmission energy that was held constant for a given spectrum. After passing through the first einzel lens, electrons were retarded by the decelerations lens and then focused by the second einzel lens to the entrance slit of the analyzer. A hole in the back plate of the electron analyzer allowed any scattered protons to pass through. On exit from the analyzer the electrons were detected by a spiraltron electron multiplier.¹⁷

Two surface barrier detectors, located at 30° and 90° with respect to the beam, were used to monitor the product of incident ion intensity and the number of target gas atoms. The yield for protons on carbon deviates from Rutherford scattering because of the non-Rutherford nuclear contribution to the elastic scattering. The necessary corrections were measured in a separate experiment by the procedure outlined by McDaniel *et al.*¹⁸

III. DATA REDUCTION AND ANALYSIS

The cross section per atom for the isotropic emission of characteristic x-rays is given by

$$\sigma_{KX} = \frac{4\pi}{L_X \Omega_X} \frac{Y_{KX}}{N_1 N_2 T F}, \quad (1)$$

where Y_{KX} is the x-ray yield from the proportional counter; L_X is the length of interaction region viewed by the proportional x-ray counter; Ω_X is the solid angle subtended by it; N_1 is the number of incident protons; N_2 is the density of the target gas atoms; T is the transparency of the window and the supporting grids; F is the fraction of characteristic x-rays absorbed in the gases of the proportional counter.

The solid angle Ω_X and the length of the interaction region L_X were calculated from the slit geometries by using a modified form of the program by Bar-Avraham and Lee.¹⁹ F depends upon the pressure of P10 gas; this fraction is adjusted to be equal to one by raising the pressure of P10 until a complete absorption of a photon in the proportional counter takes place.

$N_1 N_2$ was determined by equating the Rutherford elastic scattering cross section

$$\frac{d\sigma}{d\Omega} = 1.296 \left[\frac{Z_1 Z_2}{E_1} \right]^2 \left[\frac{1}{\sin^4(\theta/2)} - 2 \left(\frac{A_1}{A_2} \right)^2 \right] \frac{\text{mb}}{\text{sr}} \quad (2)$$

with

$$\frac{d\sigma}{d\Omega} = \frac{Y_P}{N_1 N_2 L_P \Omega_P}, \quad (3)$$

where Y_P is the particle yield which was measured by the surface barrier detector at 30° and corrected for deviations from strict Rutherford scattering. L_P and Ω_P are the length of the interaction region viewed and the solid angle

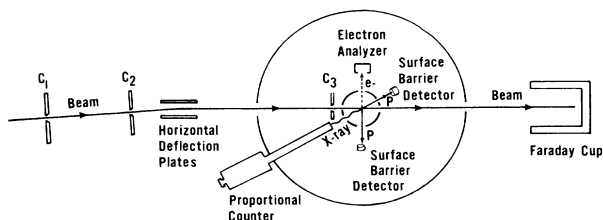


FIG. 1. Schematic diagram of the apparatus used to measure x-ray and Auger-electron cross sections.

subtended by the surface barrier particle detector. In the Rutherford formula, Eq. (2), Z_1 is the atomic number of the projectile, Z_2 is the atomic number of the K -shell ionized atom in the target gas, E_1 is the projectile laboratory energy (in MeV), and θ is the angle of scattering with respect to the beam direction in the laboratory system, A_1 and A_2 are the mass numbers of the projectile and the target atom, respectively.

Transmission of the x-ray window was measured in a separate experiment. The x-ray yield Y_{KX} and the particle yield Y_P are measured for window no. 1 of unknown transmission T_1 . Next, window no. 2 of another unknown transmission T_2 is placed in front of window no. 1; the x-ray yield Y'_{KX} and the particle yield Y'_P are measured again. From Eqs. (1) and (3), the x-ray cross section using window no. 1 is given by

$$\sigma_{KX} = \frac{4\pi}{L_X \Omega_X} \frac{d\sigma}{d\Omega} \Omega_P L_P \frac{Y_{KX}}{Y_P} \frac{1}{T_1}. \quad (4)$$

Using both windows, the x-ray cross section is given by

$$\sigma_{KX} = \frac{4\pi}{L_X \Omega_X} \frac{d\sigma}{d\Omega} \Omega_P L_P \frac{Y'_{KX}}{Y'_P} \frac{1}{T_1 T_2}. \quad (5)$$

Dividing (5) by (4), one gets the transmission of window no. 2 as

$$T_2 = \frac{Y'_{KX}/Y'_P}{Y_{KX}/Y_P}. \quad (6)$$

This window of transmission T_2 is then used for all future measurements. Such a procedure eliminates the need of measurements of solid angles, density of the target gas, and the number of incident protons. Our transmission was the same for all the gases used in this investigation and was $T_2=0.295$ for 1-MeV protons. This analysis presumes that the transmission window is the same for all projectile energies. It is conceivable that at lower energies—where multiple ionizations become increasingly important—the x-ray carbon hypersatellites of the shortest wavelengths are shifted below the absorption edge of the polypropylene window. This would result in an incomplete detection of the K -shell x rays at lower projectile energies as suggested by Toburen and Larkins²⁰ to explain the apparent decrease of K -shell fluorescence yield in carbon with the decreasing energy of the projectile. Based on our x-ray and Auger-electron measurements, we extract the fluorescence yield that shows a similar drop (some

20% in the 2–0.6-MeV range in our experiment) with the decreasing projectile energy as observed in Ref. 20. A full discussion of the carbon fluorescence yield, as a function of the multiple ionization as well as of alternations due to the molecular environment, will be made in a separate article.

Auger-electron cross section, differential in ejected electron energy, and the emission angle are given by

$$\frac{d^2\sigma_{KA}}{d\Omega dE} = \frac{Y_{KA}}{N_1 N_2 \Omega_A L_A \epsilon \Delta E_A}. \quad (7)$$

Here Y_{KA} is the number of electrons counted for N_1 protons, N_2 is the density of the target gas atoms, Ω_A and L_A are the solid angle and the length of interaction viewed by the electron analyzer, ϵ is the efficiency of the electron analyzer, ΔE_A is the spread in electron energies transmitted by the analyzer; N_1 , N_2 , Ω_A and L_A were determined by the procedure outlined above. The efficiency of the electron analyzer was fixed by comparing our 0.6-MeV proton datum on CH_4 to that measured by Stolterfoht and Schneider.²¹

Since K -shell Auger-electron emission is isotropic,²² the total cross section σ_{KA} was obtained from the double-differential cross section by integrating the area under the Auger peak to account for the energy and then multiplying $d\sigma_{KA}/d\Omega$ by 4π to account for the integration over the solid angle.

The Auger-electron spectra were recorded at a transmission energy of 100 eV. For Auger-electron measurements, pressure in the gas cell was kept below 3 mTorr to avoid any electron multiple scattering in dense target gases. The electron spectra were recorded in a multichannel analyzer and transferred to a PDP-11/34 computer system for later analysis. The Auger-electron yields for all cases were obtained by fitting a polynomial of second degree to the background regions on both sides of the peak and subtracting it from the total peak yield.

Each x-ray and Auger-electron spectrum was recorded four times to check for reproducibility. Also, each measurement was repeated on different days with very consistent results. Data were taken by keeping the energy of the proton beam constant and by recording x-ray and Auger-electron spectra after each interchange of the various carbon-based gases. Therefore, the relative error of less than $\pm 5\%$ from one gas to the next is mainly due to statistics of the Rutherford elastic scattering spectra (4%) and background subtraction (2%). The uncertainty in the

TABLE I. Measured carbon K -shell x-ray-production cross sections, σ_{KX} (kb), by protons of energy E_1 . Absolute uncertainty is $\pm 14\%$ and, at a given energy, relative uncertainty from gas to gas is $\pm 5\%$.

E_1 (MeV)	CH_4	$n\text{-C}_4\text{H}_{10}$	$i\text{-C}_4\text{H}_{10}$	C_6H_6	C_2H_2	CO	CO_2
0.6	2.45	2.25	2.23	2.16	1.99	1.77	1.78
0.8	2.34	2.16	2.17	2.06	1.90	1.68	1.71
1.0	2.27	2.06	2.05	1.98	1.85	1.63	1.67
1.2	2.19	2.00	2.01	1.93	1.78	1.56	1.60
1.4	2.12	1.91	1.92	1.85	1.72	1.52	1.55
1.6	2.02	1.85	1.84	1.76	1.66	1.47	1.48
1.8	1.97	1.81	1.80	1.72	1.60	1.42	1.44
2.0	1.91	1.76	1.77	1.67	1.56	1.38	1.40

TABLE II. Measured carbon K -shell Auger-electron-production cross sections, σ_{KA} (kb), by protons of energy E_1 . Absolute uncertainty is $\pm 16\%$ and, at a given energy, relative uncertainty from gas to gas is $\pm 5\%$.

E_1 (MeV)	CH ₄	<i>n</i> -C ₄ H ₁₀	<i>i</i> -C ₄ H ₁₀	C ₆ H ₆	C ₂ H ₂	CO	CO ₂
0.6	954	905	904	880	861	806	736
0.8	898	855	862	830	810	756	691
1.0	850	808	808	786	768	712	658
1.2	807	765	770	745	726	676	618
1.4	760	718	717	702	684	635	586
1.6	700	668	668	647	632	600	547
1.8	663	634	628	611	598	555	516
2.0	618	590	592	571	557	520	483

absolute value of the x-ray cross sections is $\pm 14\%$; it is caused by uncertainties associated with the determination of solid angle and path length (5%), transmission of the window (5%), particle-scattering spectra (4%), Rutherford differential cross section due to uncertainty in scattering angle (10%), and x-ray yield (3%). Similarly, the uncertainty in the absolute value of the Auger-electron cross sections is estimated to be $\pm 16\%$.

IV. X-RAY AND AUGER-ELECTRON-PRODUCTION CROSS SECTIONS

To reduce relative experimental errors to $\pm 5\%$, we have interchanged target gases keeping the beam energy constant. The measured x-ray, σ_{KX} , and Auger-electron, σ_{KA} , production cross sections are listed in Tables I and II, respectively; absolute uncertainties in these cross sections were, correspondingly, 14% and 16%.

Experimental molecular carbon K -shell x-ray cross sections are plotted in Fig. 2. Almost independently of the projectile energy, x-ray cross sections decrease by as much

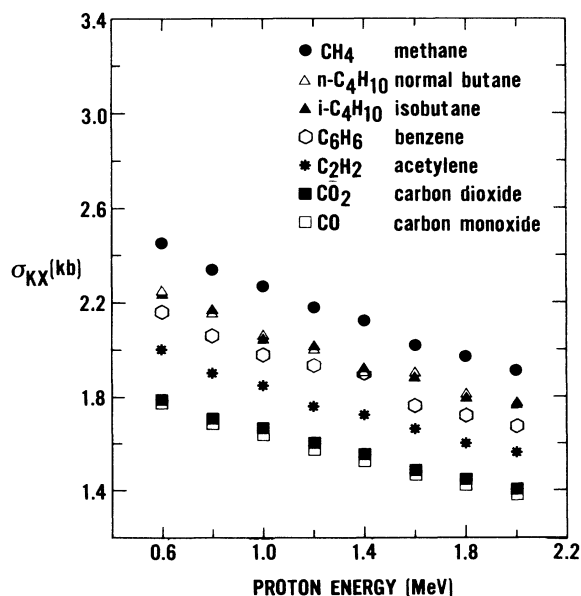


FIG. 2. K -shell x-ray-production cross sections in hydrocarbons and carbon oxides as listed in Table I. Relative uncertainties are $\pm 5\%$.

as almost 30% once CH₄ is replaced with oxides. This trend is comparable to observations of Harrison *et al.*¹ who used an electron beam instead of protons and found a 35% decrease in the relative x-ray yields from CH₄ to CO. Figure 3 gives a comparison of our carbon K -shell x-ray cross sections for methane with those of Langenberg and van Eck.¹¹ Data of Khan *et al.*⁹ for thick carbon foils and of Bissinger *et al.*¹⁰ as well as of Langenberg and van Eck¹¹ for thin carbon foils are also shown for comparison.

Carbon K -shell Auger-electron cross sections, listed in Table II, are displayed in Fig. 4 as a function of the proton energy. Similarly, as found for the x-ray cross sections but not to such a large degree, a 16% drop in these cross sections occurs when CO is substituted for CH₄. We note a decrease of about 10% from CH₄ to C₂H₂ which is comparable with the 8% change seen by Toburen.⁷ We observe also that our CO₂ cross sections are 23% lower than in CH₄ while Toburen⁷ found only an 11% decrease.

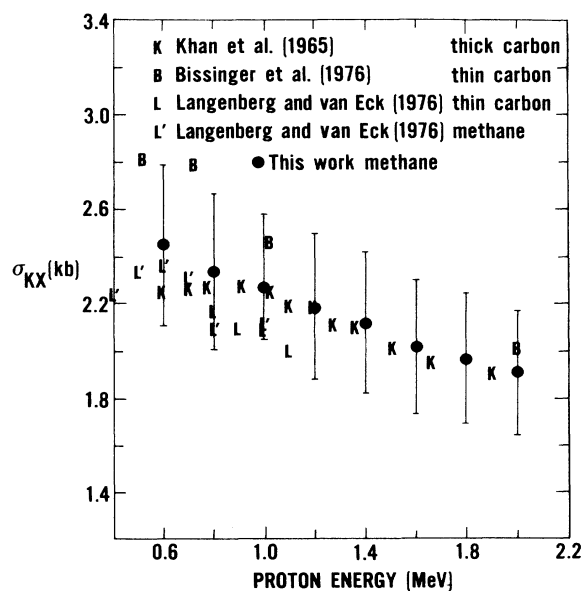


FIG. 3. K -shell x-ray production cross section in CH₄ as listed in Table I and as measured in Ref. 11. Data generated in thick (Ref. 9) and thin (Refs. 10 and 11) solid-carbon targets are displayed for comparison. Absolute uncertainties for the data of this work are $\pm 14\%$.

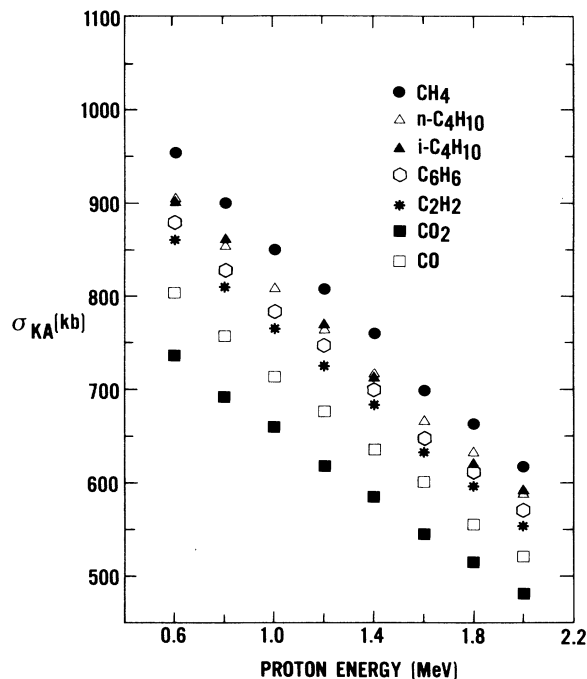


FIG. 4. *K*-shell Auger-electron-production cross sections in hydrocarbons and carbon oxides as listed in Table II. Relative uncertainties are $\pm 5\%$.

Toburen has indicated,⁷ however, that the CO and CO₂ spectra were not taken under the same conditions as the measurements for other gases. Our measurements were performed several times and also repeated using a slightly different experimental technique.²³ We have always seen about a 20% decrease after methane was replaced with carbon dioxide. We stress that it is the relative change in Auger-electron cross sections with the interchange of target gas which is of major interest. In absolute, our cross sections are typically below Toburen's measurements⁷ by some 20% for carbon *K*-shell Auger-electron production in the same gases as in Ref. 7; our carbon dioxide data are 20 to 50% below rather erratic Auger measurements of Kobayashi *et al.*²⁴ in CO₂ by 0.6–2.6-MeV protons.

Matthews and Hopkins³ have observed a 32% decrease in carbon Auger-electron cross sections for CCl₄ relative to CH₄ in 1.5-MeV proton bombardment. One of the possible explanations given by them was that the electrons could be inelastically scattered during transit through the surrounding chlorine atoms. A simple quantitative estimate was made by Matthews and Hopkins³ using a geometric expression for the probability *P* that an inelastic intramolecular scattering occurs. Their formula for *P* was specifically designed for molecules that contain only a single sulfur or carbon atom, from which Auger electrons originated, with the remaining atoms being identical. Instead of multiplying by *N*, which stands for the number of these remaining atoms, we sum the probabilities for intramolecular scattering on each of the atoms since in general the remaining atoms are different, so that

$$P = \frac{1}{2} \sum_m \{1 - \cos[\tan^{-1}(\sqrt{\sigma_m/\pi}/d_m)]\} . \quad (8)$$

Here σ_m is the total inelastic scattering cross section on the *m*th atom and d_m is the bond length to it from the atom in which Auger electrons are produced. With known²⁵ bond lengths in various carbon-bearing molecules, values of the transmission probability $1 - P$ with *P* according to Eq. (8) were calculated for the gases studied in this investigation. These transmission probabilities were obtained using known values of σ_m for inelastic scattering (i.e., ionization²⁶ plus excitation²⁷) of 270-eV (at carbon *KLL* line) electrons. Total (i.e., summed over all filled states of the atoms) inelastic cross sections for 270-eV electrons on hydrogen, carbon, and oxygen—taken as measured for ionization in Ref. 26 and calculated (using the first Born approximation) for excitation in Ref. 27—are 77, 166, and 153 Mb, respectively. With these cross sections serving as input in Eq. (8), we find the transmission factors that lower the yield of carbon *K*-shell Auger electrons, which exit from molecules, compared to what this yield would have been in atomic carbon. The transmission probabilities vary from 0.93 in CO, through 0.87 in C₂H₂, 0.86 in CO₂, 0.82 in CH₄, 0.74 in C₆H₆, to 0.73 in C₄H₁₀. This means that the Matthews and Hopkins model of intramolecular scattering predicts less than 10% percent changes relative to methane. In fact, the model indicates—contrary to our observations which give the largest Auger-electron-production cross sections in methane—that, except for polycarbon hydrocarbons, the intramolecular scattering is of larger importance in CH₄ than in any other investigated molecule. Our data for σ_{KA} (as listed in Table II) show different variations and systematics; σ_{KA} in butane, benzene, acetylene, carbon monoxide, and carbon dioxide is—practically independently of projectile energy—respectively, 95%, 92%, 90%, 84%, and 77% of σ_{KA} in CH₄. Equation (8) gives, by contrast, an opposite trend, i.e., the Auger-electron-production cross sections which are correspondingly 89%, 90%, 106%, 113%, and 105% of σ_{KA} in methane. This could signify an overestimation of the intramolecular scattering effect in methane and/or mean an underestimation of this effect in other target molecules. Such a miscalculation might result from the crudeness of the geometrical model of Ref. 3 or inaccurate inelastic cross sections that enter in this calculation; in fact, Matthews and Hopkins observe a 32% drop in Auger-electron cross sections for CCl₄ relative to CH₄ while they account in their model only for an 11% decrease.

Different transmission probabilities could have been calculated if σ_m in Eq. (8) were to be multiplied by an adjustable fitting constant, as was suggested by Varghese *et al.*²⁸ in their analysis of intramolecular scattering effects in total electron capture from molecular atoms. The adjustable fitting constant in Eq. (3) of Ref. 28 multiplies empirical electron-loss cross sections of Ref. 29 while, if it were to be introduced in our Eq. (3), such a constant would modify inelastic scattering cross sections that were adopted in our work. It is not entirely clear whether an adjustable parameter is required because theoretical excitation cross sections²⁷ are too low for O (hydrogenic wave functions used in these calculations might not be as suit-

able for oxygen as for H). For consistency, however, carbon cross sections would have to be increased as well. This would result in even larger disagreement with our data for polycarbon molecules. Crudeness of the geometrical model in the transmission-probability calculations might be alternatively a rationale for an adjustable constant; perhaps a physical model of intramolecular scattering that accounts for diffraction effects³⁰ could eliminate the need for such modifications. Still, there is no single adjustable constant that would multiply the assumed σ_m in Eq. (8) to fit *comprehensively* our experimental findings. The data impose constraints on the cross sections used in Eq. (8). To explain the observed trends in *all* target molecules, one would have—keeping the oxygen cross sections intact—to assume about half as small a cross section for inelastic scattering on carbon atoms and to stipulate that hydrogen atoms have virtually no effect on intramolecular scattering. We believe that such assumptions are realistic because the Auger electrons that scatter on hydrogen can at most suffer a 13.6-eV energy loss and similarly small energy losses are involved in excitation of carbon electrons. The scattered 270-eV electron loses typically in such collisions less than 5% of its energy and thus most probably falls into the energy window of the detector just as likely as any unscattered Auger electron. By contrast in ionization *as well as excitation* of oxygen, the intramolecularly scattered electron suffers an energy loss which is sufficiently large so that this electron eludes the detection. Hence, with no change in the calculated transmission probabilities of the carbon *K*-shell Auger electron through carbon oxides, we apply Eq. (8) again to revise the transmission probabilities in all hydrocarbons. We repeat the calculation setting σ_m for hydrogen scattering equal to zero and reducing the inelastic cross section for carbon to 88 Mb, which is its ionization part only. The recalculated transmission probabilities for hydrocarbons are 0.90 in C_6H_6 , 0.95 in C_4H_{10} , and 0.96 in C_2H_2 . With $\sigma_m = 0$ for H, there is no intramolecular correction in CH_4 . All calculated transmission probabilities are now consistent with the trends exhibited in measured variations of Auger-electron production in molecular carbon.

To focus on one molecule, Fig. 5 gives a comparison of our Auger-electron cross sections for CH_4 to those measured by Toburen,⁷ Stolterfoht and co-workers,^{21,22} and Rødbro *et al.*³¹ All data in Fig. 5 are for CH_4 with the exception of 1.5- and 2.0-MeV cross sections of Toburen that are averages of his data for hydrocarbon gases other than methane. Our Auger-electron-production cross section by 1-MeV protons in methane is significantly lower than that published by Toburen because we chose to normalize our measurements to the 0.6-MeV measurement of 954 kb in CH_4 by Stolterfoht and Schneider.²¹ Rødbro *et al.*³¹ have chosen a value of 1010 kb at 0.5 MeV proton impact—which is 9% larger than we would extrapolate from our data or deduce from Ref. 21—to normalize all the data of Ref. 31. Auger-electron cross sections of the present work between 0.6 and 1.0 MeV for CH_4 are, within the error bars, identical to those published earlier³² and concurrently also in other molecules^{23,33} by Toten *et al.*; in particular, carbon *K*-shell Auger-electron-production cross sections are found^{23,33} 19% lower in CO_2

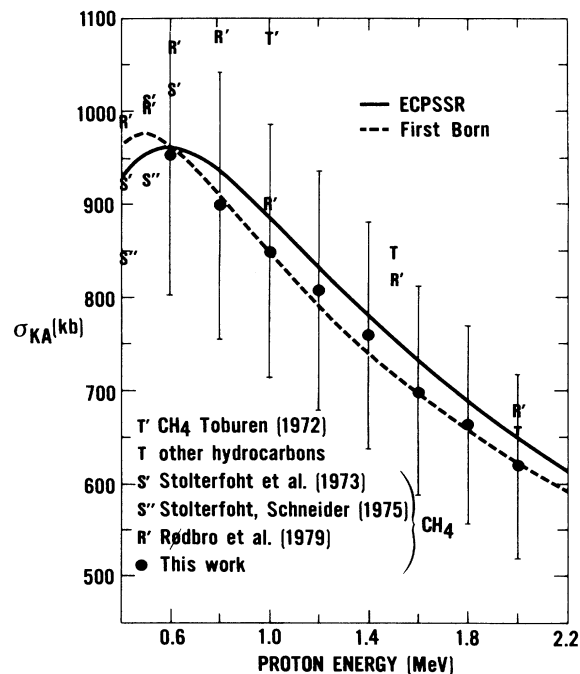


FIG. 5. *K*-shell Auger-electron-production cross section in CH_4 as listed in Table II and as measured in Refs. 7, 21, 22, and 31; Toburen's data at 1.5 and 2.0 MeV represent averages of cross sections measured on hydrocarbons other than methane. The first Born (dashed curve) of Ref. 12 and ECPSSR (solid curve) of Ref. 13 were calculated using 290.6 eV, the *K*-shell binding energy for carbon in methane; no corrections for intramolecular scattering were made to calculate these curves. Absolute uncertainties for the data of this work are $\pm 16\%$.

than in CH_4 .

Our Auger-electron data on CH_4 as a function of proton energy are compared to the first Born¹² and ECPSSR (Ref. 13) theories in Fig. 5. The contribution of the electron capture by protons to the target ionization was small (calculated¹³ to be less than 6%) in the energy range of our data. Since the Auger yield $1 - \omega_K = 0.998$ is nearly equal to 1.0 for carbon, one can equate the Auger-electron cross section σ_{KA} with the ionization cross section σ_K . Our data for CH_4 are in relatively good agreement with both the first Born and ECPSSR calculations; in fact, the agreement is very good with the first Born which might be somewhat accidental in view of 16% ambiguities in absolute normalization of the data. Neither of these calculations was designed to treat ionization of molecular carbon in an *ab initio* molecular approach. As Matthews and Hopkins conclude³ "atomic vacancy production cannot necessarily be deduced from Auger-electron measurements which have been performed using molecular targets."

Effects of chemical environment can be categorized as "entrance" and "exit" effects within the molecule;³⁴ the former stems from the changed binding energy and occupation number of the *K* shell in molecular carbon while the latter effect results from intramolecular scattering on the exit through the target molecule. The entrance effect

is of relatively small importance in affecting ionization of tightly bound electrons in the ground state of carbon. Self-consistent calculations of molecular wave functions³⁵ prove that in fact the $1s$ state remains populated by 2.00 electrons for carbon in a variety of molecules. Chemical shifts away from the observed binding energy of 283.8 eV in the atomic carbon³⁶ can be deduced from experimental values in carbon-bearing molecules. It is known³⁷ that these values are linearly related to the Pauling charge, q_p , which is defined in terms of the ionic electronegativities;³⁸ Fig. 5.4.8 of Ref. 37 clearly indicates that the carbon K -shell binding energy $\hbar\omega_{2K}$ versus q_p can be fitted well by a straight line. Our least-squares fit gives (291.7 eV) $(1 + 0.0225q_p)$, which within 0.3% approximates available empirical values for the carbon K -shell binding energy in molecules. The first Born and ECPSSR curves in Fig. 5 were calculated using 290.6 eV of our least-squares fit with $q_p = -0.16$ for CH_4 ; they are at most 5% lower than the calculations performed with 283.8 eV as ascribed to atomic carbon in Ref. 36. Even for CO_2 in which the K -shell level of carbon is shifted the most relative to that in methane, a relative increase in the binding energy is only 2.4%. Given the rather weak dependence of ionization cross sections on $\hbar\omega_{2K}$ [$\sigma_K \propto (\hbar\omega_{2K})^{-p}$ with p between 2.0 for 0.6-MeV and 1.6 for 2.0-MeV protons], the entrance effect could explain at most a 5% decrease of σ_{KA} in CO_2 relative to CH_4 at the lowest proton energy for our data. This 5% decrease due to the chemical shift is combined with the exit effect—which was a 14% decrease as calculated above with revised input cross sections in the Matthews and Hopkins model of intramolecular scattering—so that we estimate a 20% decrease for Auger-electron cross sections in CO_2 relative to CH_4 . This is in excellent agreement with what is seen in our data.

Encouraged by such an agreement, we propose to revisit the original interpretation of the 32% decrease in Auger-electron cross sections for CCl_4 relative to CH_4 seen by Matthews and Hopkins in their data.³ It appears that the transmission probability of 0.83 in CCl_4 that these authors calculated was too high because *only* ionization cross section of Ref. 26 served as an input in its evaluation. We do not see any justification for the neglect of excitation in Cl after which the scattered electron suffers sufficiently large energy losses to fall outside the detector's window. Based on growing (with the increasing atomic number) contribution of excitation to inelastic cross sections, we extrapolate that the inelastic cross section for scattering of 270-eV electrons on chlorine is 1.6 times larger than the ionization cross section. Thus the inclusion of excitations would lower the transmission probability in CCl_4 to 0.73. In gauging the Auger-electron production in tetrachloro-carbon by the same process in methane, we assume that no effective intramolecular scattering occurs in CH_4 , i.e., although scattered within the methane molecule, the carbon Auger electrons pass fully through the energy window of the detector; since this assumption was not made by Matthews and Hopkins they would find 0.92 instead 1.0 for the transmission probability in methane. Hence on account of the intramolecular scattering exit effect we find that the carbon K -shell Auger-electron cross section in

CCl_4 is 27% lower than in CH_4 instead of just the 11% calculated in Ref. 3. After further reduction of the cross section in CCl_4 relative to CH_4 by some 5% due to the entrance effect, we obtain again excellent agreement with the experiment.

In conclusion, carbon K -shell ionization cross sections obtained as a series of Auger-electron-production measurements in various hydrocarbons and carbon oxides are dependent on the molecular environment of carbon. Such dependence is attributed primarily to intramolecular scattering. The simple model of Matthews and Hopkins³ fails to predict this dependence even qualitatively. This occurs when the carbon Auger electrons, in addition to being scattered through ionization of the remaining carbon atoms within the molecule, are thought to be dislocated out of the detector's view via excitations. Also, the model of Ref. 3 leads to wrong predictions when the intramolecular scattering contribution of hydrogen atoms is included. We argue that excitations of carbon atoms and inelastic collisions on hydrogen atoms are unable to eliminate the scattered Auger electron from the detector's window. The intramolecular scattering, as calculated with an effective neglect of H atoms and with the disregard for the collisions which cause excitations of C atoms, lowers the ionization cross sections in CO_2 relative to CH_4 to the same degree as seen in our data after changes due to the chemical shift of K -shell binding energy are also accounted for. Excitations, however, do contribute to the effective intramolecular scattering on oxygen and certainly chlorine atoms. In fact, the added excitation cross section in a full account of inelastic scattering on Cl atoms has removed a jarring discrepancy between the model and the data of Ref. 3. Thus it was not the model but the employed cross section that was at a source of this discrepancy.

X rays that emerge from carbon in the aftermath of its ionization reflect only the entrance-effect differences in ionization cross sections. It is the rate of their production which, relative to nonradiative transition rates, can be largely enhanced by the distortion of carbon atoms in molecules. This change in the fluorescence yield is a primary source of variations of σ_{KX} in different molecules. Carbon-monoxide data present an exception; apparently the carbon fluorescence yield is not enhanced in CO as much as in other molecules. Auger-electron cross sections in CO lie above σ_{KA} in CO_2 (see Fig. 4). In x-ray measurements (see Fig. 2), however, carbon cross sections in CO are smaller than in other molecules because the increase of the fluorescence yield in carbon of CO is minute relatively to the modifications of fluorescence yield that occur in other molecules. Changes in the carbon K -shell x-ray-production cross section for different target molecules are typically larger than the molecular variations that we have discussed above; this is because the fluorescence yields—knowledge of which was irrelevant in the Auger-electron cross-section analysis because $\omega_K \ll 1$ for carbon—are indeed quite sensitive to the molecular milieu of the carbon atom. Variations in ω_K and their explanation as well as the observed lack of variations in CO will be discussed in a separate article where these changes are to be correlated with molecular distortions of the carbon L shell.

ACKNOWLEDGMENTS

We thank L. H. Toburen for a copy of the program of Bar-Avraham and Lee to calculate the product of the solid angle and the length of interaction seen by the various detectors. We also wish to acknowledge R. L. Watson

and K. Parthasarathi for providing polypropylene used in the proportional counter window. This work was supported in part by the Robert A. Welch Foundation and the North Texas State University Organized Research Fund and is a part of the Ph.D. requirements for one of the authors (R.P.B.).

- *Present address: Department of Physics, Idaho State University, Pocatello, Idaho 83209.
- ¹K. G. Harrison, H. Tawara, and F. J. de Heer, *Chem. Phys. Lett.* **14**, 285 (1972); *Physica* **63**, 351 (1973).
 - ²G. Bissinger, J. M. Joyce, J. A. Tanis, and S. L. Varghese, *Phys. Lett.* **77A**, 156 (1980).
 - ³D. L. Matthews and F. Hopkins, *Phys. Rev. Lett.* **40**, 1326 (1978).
 - ⁴R. P. Chaturvedi, D. J. Lynch, L. H. Toburen, and W. E. Wilson, *Phys. Lett.* **61A**, 101 (1977).
 - ⁵H. Endo, M. Uda, and K. Maeda, *Phys. Rev. A* **22**, 1436 (1980).
 - ⁶R. L. Watson, T. Chiao, and F. E. Jenson, *Phys. Rev. Lett.* **35**, 254 (1975).
 - ⁷L. H. Toburen, *Phys. Rev. A* **5**, 2482 (1972).
 - ⁸D. Burch, N. Stolterfoht, D. Schneider, H. Wieman, and J. S. Risley, *Phys. Rev. Lett.* **32**, 1151 (1974); G. Wüstefeld, D. Schneider, P. Ziem, and N. Stolterfoht, Fifth International Conference on Vacuum Ultraviolet Radiation Physics, Montpellier, France, 1977 (unpublished).
 - ⁹J. M. Khan, D. L. Potter, and R. D. Worley, *Phys. Rev. A* **139**, 1735 (1965).
 - ¹⁰G. Bissinger, J. M. Joyce, and H. W. Kugel, *Phys. Rev. A* **14**, 1375 (1976).
 - ¹¹A. Langenberg and J. van Eck, *J. Phys. B* **9**, 2421 (1976).
 - ¹²G. S. Khandelwal, B.-H. Choi, and E. Merzbacher, *At. Data Tables* **1**, 103 (1969); R. Rice, G. Basbas, and F. D. McDaniel, *At. Data Nucl. Data Tables* **20**, 503 (1977) for direct ionization; V. S. Nikolaev, *Zh. Eksp. Teor. Fiz.* **51**, 1263 (1966) [*Sov. Phys.—JETP* **24**, 847 (1967)] for electron capture.
 - ¹³W. Brandt and G. Lapicki, *Phys. Rev. A* **23**, 1717 (1981) for direct-ionization calculations; G. Lapicki and F. D. McDaniel, *ibid.* **22**, 1896 (1980); **22**, 975(E) (1981) for electron-capture calculations. The ECPSSR cross sections, as the first Born approximation cross sections of Ref. 12, are calculated as sums of direct-ionization and electron-capture cross sections.
 - ¹⁴Purchased from L. E. Pink Engineering Ltd., Reading, England.
 - ¹⁵Purchased from Emerson & Cumming, 604 West 182 St., Gardena, CA 90248.
 - ¹⁶A. Toten, F. Breyer, A. Hamdi, R. P. Bhalla, and F. D. McDaniel, *IEEE Trans. Nucl. Sci.* **NS-28**, 1567 (1981).
 - ¹⁷Galileo Electro-Optics Corp., Galileo Park, Sturbridge, MA 01518.
 - ¹⁸F. D. McDaniel, T. J. Gray, R. K. Gardner, G. M. Light, J. L. Duggan, H. A. Van Rinsvelt, R. D. Lear, G. H. Pepper, J. W. Nelson, and A. R. Zander, *Phys. Rev. A* **12**, 1271 (1975).
 - ¹⁹E. Bar-Avraham and L. C. Lee, University of Southern California Report No. USC-136-138 1968 (unpublished).
 - ²⁰L. H. Toburen and F. P. Larkins, *Phys. Rev. A* **5**, 2482 (1972).
 - ²¹N. Stolterfoht and D. Schneider, *Phys. Rev. A* **11**, 721 (1975).
 - ²²N. Stolterfoht, D. Schneider, and K. G. Harrison, *Phys. Rev. A* **8**, 2363 (1973).
 - ²³A. Toten, Ph.D. thesis, North Texas State University, Denton, Texas, 1986 (unpublished).
 - ²⁴N. Kobayashi, N. Maeda, H. Hori, and M. Sakisaka, *J. Phys. Soc. Jpn.* **40**, 1421 (1976); N. Kobayashi, T. Irie, N. Maeda, H. Kojima, S. Akanuma, and M. Sakisaka, *ibid.* **47**, 234 (1979).
 - ²⁵*Tables of Interatomic Distances and Configurations in Molecules and Ions*, Special Publication No. 11, edited by L. E. Sutton, (Chemical Society, London, 1958).
 - ²⁶D. Rapp and P. Englander-Golden, *J. Chem. Phys.* **43**, 1464 (1965).
 - ²⁷V. A. Pitkevich and V. G. Videnskii, *At. Energ.* **40**, 311 (1976) [*Sov. At. Energy* **40**, 382 (1976)].
 - ²⁸S. L. Varghese, G. Bissinger, J. M. Joyce, and R. Laubert, *Phys. Rev. A* **31**, 2022 (1985).
 - ²⁹L. H. Toburen, M. Y. Nakai, and R. A. Langley, *Phys. Rev.* **171**, 562 (1966).
 - ³⁰G. Lapicki, *Bull. Am. Phys. Soc.* **29**, 817 (1984).
 - ³¹M. Rødbro, E. Horsdal Pedersen, C. L. Cocke, and J. R. MacDonald, *Phys. Rev. A* **19**, 1936 (1979).
 - ³²F. D. McDaniel, A. Toten, R. P. Bhalla, and G. Lapicki, *Nucl. Instrum. Methods A* **240**, 492 (1985); A. Toten, F. D. McDaniel, and G. Lapicki, *Nucl. Instrum. Methods B* **10/11**, 150 (1985).
 - ³³A. Toten, F. D. McDaniel, and G. Lapicki (unpublished).
 - ³⁴G. Bissinger, J. M. Joyce, G. Lapicki, R. Laubert, and S. L. Varghese, *Phys. Rev. Lett.* **49**, 318 (1982).
 - ³⁵L. C. Snyder and H. Basch, *Molecular Wave Functions and Properties: Tabulated from SCF Calculations in a Gaussian Basis Set* (Wiley, New York, 1972).
 - ³⁶J. A. Bearden and A. F. Burr, *Rev. Mod. Phys.* **39**, 125 (1967).
 - ³⁷K. Siegbahn, C. Nordling, G. Johansson, S. Hedman, P. F. Hadén, K. Hamrin, V. Gelius, T. Bergmark, L. O. Werme, R. Manne, and Y. Baer, *ESCA Applied to Free Molecules* (North-Holland, Amsterdam, 1971).
 - ³⁸L. Pauling, *College Chemistry*, 3rd edition (Freeman, San Francisco, 1964).